High-Precision Strain Measurement Bridge Circuit With On-line Compensation for Parasitic Capacitance Effects

Masashi Kono † Tetsuya Taura † Takahide Suzuki † Hiroshi Sunaga † Yoshihisa Yamada †
Keigo Kimura † Masanao Morimura †† Haruki Okano ††† Masami Iwasaki †††
Hiroyuki Takuno ††† Mitsumasa Suzuki ††† Yukio Shinoda ††† Haruo Kobayashi †

† Dept. of Electronic Engineering, Graduate School of Engineering, Gunma University
1-5-1 Tenjin-cho, Kiryu Gunma 376-8515,Japan.
†† Consultant, 202-570 18th St. West Vancouver, B.C. V7V 3V7 ,Canada.
††† Tokyo Sokki Kenkyujo Co., Ltd., 4-247 Aioi-cho Kiryu Gunma 376-0011,Japan.

E-mail : {kono,h_haruo}@el.gunma-u.ac.jp

ABSTRACT

This paper describes a high-precision strain measurement system using modern ADC and digital technology to provide real-time compensation for parasitic capacitance effects. In recent applications, strain gauges used for strain measurement often have to be located far from strain measuring instruments, requiring long connecting cables with associated parasitic capacitance; in such cases the parasitic capacitance degrades measurement accuracy significantly, and parasitic capacitance variation can cause measurement drift. The proposed algorithm can reliably and accurately compensate for parasitic capacitance in the digital domain both for one-gauge and two-gauge systems. We have demonstrated its effectiveness by simulation and experiments using field data.

Keywords: *Strain Measurement, Strain Gauge, Bridge Circuit, Calibration.*

1. Introduction

Recently much attention is being paid to sensor technology for automotive applications. In this paper we focus on high-precision strain measurement technology (Figs.1, 2 and 3, [1]-[9]) for such applications. Strain measurement methods can be classified into DC (Fig.4) and AC (Fig.5) methods. DC methods are simple, but suffer from low-frequency noise (such as 50Hz or 60Hz hum noise from power supply), drift, and thermal electromotive force (emf), and hence cannot achieve high precision. On the other hand, while AC methods are not affected by low-frequency noise, drift, and thermal emf, they suffer from parasitic capacitance effects (Fig.6,[1]). In this paper, we describe how we have attempted to solve this problem of parasitic capacitance effects, which have been a problem for a long time in AC methods of strain measurement, for both one-gauge and two-gauge systems, using ADC and modern digital technology.

2. Principle of Strain Measurement with Strain Gauge and Bridge Circuit

When a material is stretched (or compressed), the force used generates a corresponding stress σ inside the material. This stress in turn generates a proportional tensile strain (or compressive strain) which deforms the material by $L + \Delta L (or L - \Delta L)$,where L is the original length of the material. When this occurs, the strain is the radio of ΔL to L (Fig.1).

$$\varepsilon = \frac{\Delta L}{L} = \frac{1}{k}\frac{\Delta R}{R}. \tag{1}$$

Fig.2 shows an example of a strain gauge and a Wheatstone bridge circuit; there are several types of their combinations according to applications. Suppose that the applied strain changes the gauge resistance from R to $R + \Delta R$. Then the Wheatstone bridge circuit output voltage ΔV is given by

$$\begin{aligned} \Delta V &= \left(\frac{1}{2} - \frac{R}{2R + \Delta R}\right) \cdot V_{in} \\ &= \frac{1}{2} \cdot \frac{\frac{\Delta R}{R}}{2 + \frac{\Delta R}{R}} \cdot V_{in}, \end{aligned}$$

and we can obtain the strain value ε as

$$\begin{aligned} \varepsilon &= \frac{2}{k} \cdot \frac{2\Delta V}{V_{in} - 2\Delta V} \\ &= \frac{2}{k} \cdot \frac{\frac{2\Delta V}{V_{in}}}{1 - \frac{2\Delta V}{V_{in}}} \simeq \frac{2}{k} \cdot \frac{2\Delta V}{V_{in}}. \end{aligned}$$

Usually $k = 2, V_{in} = 2[V]$ are used.

3. Analysis of Parasitic Capacitance Influences

In applications where the strain gauge must be at some distance from the strain measuring instrument, and so long wires must be used to connect them, the parasitic capacitance associated with the wires limits the accuracy of the measurement (Fig.6). In this section we analyze the parasitic capacitance effects.

3.1 Quarter Bridge 2-wire System (Fig.2)

Fig.2 (a) shows Wheatstone bridge circuit with one strain gauge, while Fig.2(b) shows its equivalent circuit with parasitic capacitance, and we have derived its transfer function $H(j\omega)(= V_{out}(j\omega)/V_{in}(j\omega))$:

$$H(j\omega) = H_{RE}(\omega) + jH_{IM}(\omega). \quad (2)$$

Here

$$H_{RE}(\omega) = \frac{1}{2}\cdot\frac{x(2+x) - \omega^2R^2C^2(1+x)^2}{(2+x)^2 + \omega^2R^2C^2(1+x)^2}. \quad (3)$$

$$H_{IM}(\omega) = \frac{-\omega RC(1+x)^2}{(2+x)^2 + \omega^2R^2C^2(1+x)^2}. \quad (4)$$

$$R' = R + \Delta R, \qquad x = \frac{\Delta R}{R}. \quad (5)$$

3.2 Half Bridge System (Fig.3)

When we use a two-gauge system, we can have information whether the strain is due to "stretch" or "bending" of a specimen. (On the other hand a one-gauge system cannot provide such information). A two-gauge system has two configurations; two gauges can be placed right next to each other in the bridge circuit (Fig. 3), or opposite side of each other. Also it has several gauge-attachment methods to the specimen; one method is that the one gauge is attached to the specimen and the othe is to the dummy specimen (1-active-1-dummy method), which can compensate for temperature drift and cable resistance effects. Also two gauges can be attached to the one side of the specimen (Fig.7) or both sides (Fig.8).

Fig.3(a) shows a Wheatstone bridge circuit with two strain gauges, while Fig.3 (b) shows its equivalent circuit with parasitic capacitances, and we have derived its transfer function $H(j\omega)$:

$$H(j\omega) = H_{RE}(\omega) + jH_{IM}(\omega). \quad (6)$$

Here

$$H_{RE}(\omega) = \frac{1}{2D(\omega)}\cdot\Big((2+x_1+x_2)(x_1-x_2) + \omega^2R^2(1+x_1)^2(1+x_2)^2 \times(C_2+C_1)(C_2-C_1)\Big). \quad (7)$$

$$H_{IM}(\omega) = \frac{\omega R(1+x_1)(1+x_2)}{D(\omega)} \quad (8)$$

$$\times \{C_2(1+x_2) - C_1(1+x_1)\}. \quad (9)$$

$$D(\omega) = (2+x_1+x_2)^2 + \omega^2R^2(1+x_1)^2(1+x_2)^2(C_1+C_2)^2. \quad (10)$$

$$R_1 = R + \Delta R_1, \qquad x_1 = \frac{\Delta R_1}{R}. \quad (11)$$

$$R_2 = R + \Delta R_2, \qquad x_2 = \frac{\Delta R_2}{R}. \quad (12)$$

According to the gauge-attachment methods, x_1 and x_2 are defind as follows:

- 1-active-1-dummy method case:

$$x_1 = x, \qquad x_2 = 0. \quad (13)$$

- Two-active method case I (Fig.7):

$$x_1 = x, \qquad x_2 = \nu x. \quad (14)$$

  Here, ν is the Poisson ratio (which is a given value and in many cases $\nu \approx 0.3$).

- Two active method case II (Fig.8):

$$x_1 = x, \qquad x_2 = -x. \quad (15)$$

In the case of half bridge system, the number of unknown parameters (ε, C_1, C_2) is three. We see that both the real and imaginary parts of $H(j\omega)$ are affected by parasitic capacitances C_1, C_2 (Fig.9) .

4. Conventional Strain Measurement Method and its Problem

A conventional AC dynamic strain measurement system measures only the real part $H_R(j\omega)$ of the bridge output voltage by analog phase detection circuit and calculates the strain, assuming that C_1, C_2 are small enough to be neglected. (Also that ε squared and ε cubed are neglected.) However, in recent applications where parasitic capacitances are not negligible due to long wires from gauges to a bridge circuit (Fig.6) and very high precision measurement is demanded, these assumptions are not valid any more. Sometimes an analog calibration method (capacitance balance circuit) is used to compensate for parasitic capacitances as shown in Fig.10, but due to temperature change and aging effects this method cannot satisfy more demanding requirements.

5. Proposed Parasitic Capacitance Cancellation System

5.1 Configuration

Fig.11 shows our proposed strain measurement system, and it has the following features:
(a) Oscillators of two different frequencies (ω_1) is used. ($\omega_1/2\pi$) is on the order of 10kHz.
(b) The bridge output is amplified by an AC amplifier which does not suffer from low frequency noise.
(c)The input and output signals of the bridge circuit are converted to digital data (with accuracy of 16 bits or greater) by delta-sigma modulators, and are stored in memory.
(d)A digital signal processor compensates for parasitic capacitance C and calculates ε.

5.2 Algorithm

Our strain calculation algorithm is as follows:
(1) The input $cos(\omega_1 t)$ is applied to the bridge circuit, and its input and output are converted to digital signals. Digital filter operation is performed to them so that the component of $cos(\omega_1 t)$ is extracted from the input part and also ω_1 component is obtained from the output. By multiplying the input $cos(\omega_1 t)$ and output ω_1 component signal, and taking the time average of the multiplication result in the digital domain, we have the value of $H_{RE}(\omega_1) = V_{cr1}$.
In other words, if the output ω_1 component signal $V_{out}(t) = a_1 cos(\omega_1 t) + b_1 sin(\omega_1 t)$,

$$\begin{aligned} cos(\omega_1 t) \times V_{out}(t) &= \frac{a_1}{2} + \frac{a_1}{2} cos(2\omega_1 t) \\ &+ \frac{b_1}{2} sin(2\omega_1 t), \\ then \quad H_{RE}(\omega_1) &= \frac{a_1}{2} = V_{cr1}. \end{aligned} \tag{16}$$

(2) In the same way, the input $cos(\omega_1 t)$ is applied to the bridge circuit, and its input and output are converted to digital signals. Digital filter operation is performed to them so that the component of $cos(\omega_1 t)$ is extracted from the input part and also ω_1 component is obtained from the output. The input $cos(\omega_1 t)$ is phase-shifted by 90 degrees in the digital domain, to obtain $sin(\omega_1 t)$ precisely (Accurate 90-degree phase-shift in digital domain is one of advantages of our proposed system.) Then by multiplying $sin(\omega_1 t)$ and the output ω_1 component, and taking the time average of the multiplication result in the digital domain, we have the value of $H_{IM}(\omega_1) = V_{ci}$.

$$\begin{aligned} \sin(\omega_1 t) \times V_{out}(t) &= \frac{b_1}{2} - \frac{b_1}{2} \cos(2\omega_1 t) \\ &+ \frac{a_1}{2} \sin(2\omega_1 t), \\ \text{then} \quad H_{IM}(\omega_1) &= \frac{b_1}{2} = V_{ci}. \end{aligned} \tag{17}$$

$H_{RE}(\omega_1)$ and $H_{IM}(\omega_1)$ are defined by eqs. (3) and (4) respectively. Note that a_1, b_1 can be obtained also by the curve fitting algorithm [10], as described later.

Since the number of unknown variables (C_1, x) is two for the one-gauge system, and we have two equations,(16),(17), hence we can obtain x by cancelling C_1, and then we have the strain value ε using eq.(1). Note that we have the third-order polynomial equation of x when we cancel C_1, but we can have its accurate solution by digital numerical calculation.

For the two-gauge system, we apply also the input singal of a different frequency ω_2, and we can have four equations.

5.3 Advantages of our Digital Method

Parasitic capacitance values are unknown and can change according to temperature and aging. Analog signal processing circuits may generate additional noises inside them. However the above-mentioned system and algorithm are digital, and they can reliably compensate for parasitic capacitance on-line. Delta-sigma ADCs with greater than 16bit accuracy and a few tens kilo Hertz bandwidth are now commercially available, and which, together with recent rapid progress of DSP, enable realization of our proposed system at low cost.

In practical usage, we plan to cancel the parasitic capacitance effects roughly by the analog capacitance circuit (Fig.10), and its temperature drift parts precisely by the proposed digital method.

6. Evaluation of Proposed Algorithm Using Field Data

We have evaluated the proposed algorithm using the actual field data for one gauge system (Fig.12).
(i) We have applied a sinusoidal input of 5kHz (or 20kHz) to the bridge circuit with parasitic capacitances of 1,000pF (or 3,000pF), and the bridge circuit output is fed to the following AC amplifier.
(ii) We have collected AD-converted input data to the bridge circuit, and AD-converted output data of

the AC amplifier using a strain measurement instrument. Note that we do not have to implement hardware of digital processing parts for its evaluation, and calculation by software is enough for that purpose.
(iii) We have estimated the amplitudes and phases of the actual input and output sine waves using a sine curve fitting algorithm which we have developed with C program [10], and obtained the real imaginary part values of the transfer function.
(iv) We have calculated the strain and the parasitic capacitance values using the obtained values and the proposed algorithm.
(v) We have also calculated the strain value using the conventional algorithm (which uses only the real part and ignores the parasitic capacitance).
(vi) We have compared the results calculated by the proposed and conventional algorithms, and confirmed the precision of the proposed algorithm.

Table.1 shows the calculation results using field data. X-axis indicates the parasitic capacitance value, and Y-axis shows an error from the true strain value ($10,000\mu\varepsilon$). We see that the proposed algorithm reduces the error from 1.4 % to 0.5 % with parasitic capacitance value of 3,000pF and input frequency of 5kHz, and from 49 % to 3.4 % with parasitic capacitance value of 3,000pF and input frequency of 20kHz.

Table 1. Accuracy comparison of strain measurement between proposed and conventional algorithms using field data. (Strain value = $10,000[\mu\varepsilon]$).

Paracitic capacitance	Input frequency	Error (conventional)	Error (proposed)
1,000 [pF]	5[kHz]	1.5[%]	0.8[%]
3,000 [pF]	5[kHz]	1.4[%]	0.5[%]
1,000 [pF]	20[kHz]	5.0[%]	0.6[%]
3,000 [pF]	20[kHz]	49.5[%]	3.4[%]

7. Conclusions

We have proposed a high-precision strain measurement system based on modern ADC and digital technology. In recent applications strain gauges have to be put on objects under strain measurement far from strain measurement instruments, which require long lines with associated parasitic capacitances; in such cases parasitic capacitances degrade measurement accuracy significantly and cause drift. The proposed algorithm can cancel them on-line in digital domain, which is reliable and accurate. We have demonstrated its effectiveness by simulation and experiment using field data.

Acknowledgement We would like to thank Prof. H. Yamasaki, Mr. I. Tazawa and Mr. K. Wilkinson for valuable comments.

References

[1] M. Kono, T. Taura, T. Suzuki, H. Sunaga, Y.Yamada, K. Kimura M. Morimura、H. Okano, M. Iwasaki, H. Takuno, M. Suzuki、 Y. Shinoda, H. Kobayashi "A High-Precision Strain-Measurement Bridge Circuit System with On-line Digital Calibration ", Circuits and Systems Workshop in Karuizawa, (April, 2007).

[2] T. Taura, M. Kono, H. Sunaga, K. Kimura, M. Morimura, H. Okano, M. Iwasaki, H. Takuno, M. Suzuki, H. Kobayashi, "High-Precision Strain Measurement Bridge Circuit System", The 23th Sensing Forum,The Society of Instrument and Control Engineers, (Oct. 2006).

[3] M. Kono, T. Taura, H. Sunaga, K. Kimura, T. Suzuki, M. Morimura, H. Okano, M. Iwasaki, H. Takuno, M. Suzuki, H. Kobayashi,"A High-Precision AC Wheatstone Bridge Strain Gauge ", 2006 IEEJ International Analog VLSI Workshop, Hangzhou,China (Nov. 2006).

[4] J. J. Carr, Elements of Electronic Instrumentation and Measurement, Third Edition, Prentice Hall (1996).

[5] McGraw-Hill Concise Encyclopedia of Science and Technology, McGrawHill (1998).

[6] B. Liptak, Instrument Engineer's Handbook, Process Measurement and Analysis CRC Press LLC (1995).

[7] Analog Devices Inc. Op Amp Applications, CQ Publishing (2003).

[8] Omegadyne Pressure, Force, Load, Torque Databook, Omegadyne Inc. (1996).

[9] Strain Gauge Users' Guide, Tokyo Sokki Kenkyujo Co. Ltd.

[10] Y. Motoki, H. Sugawara, H. Kobayashi, T. Komuro, and H. Sakayori, " Multi-Tone Curve Fitting Algorithms for Communication Application ADC Testing, " Electronics and Communication in Japan: Part II: Electronics, Wiley Periodicals Inc. vol.86, no.8, pp.1-11 (2003).

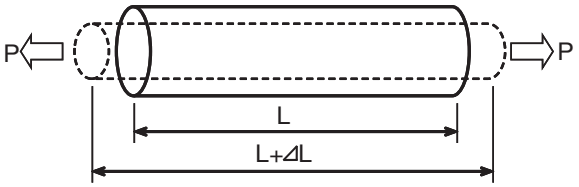

Fig. 1. Explanation of "Strain".

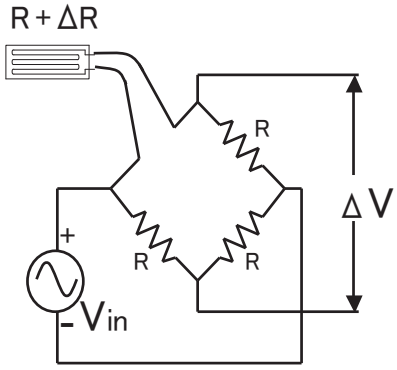

(a)

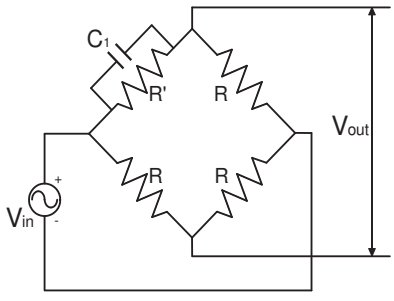

(b)

Fig. 2. (a) Strain gauge and Wheatstone bridge circuit (quarter bridge 2-wire system). (b) Bridge circuit with parasitic capacitance.

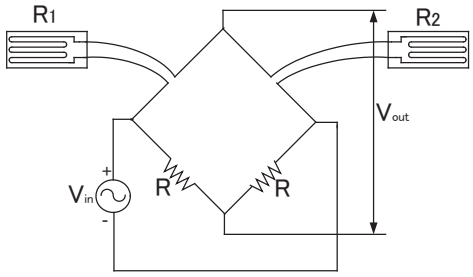

(a)

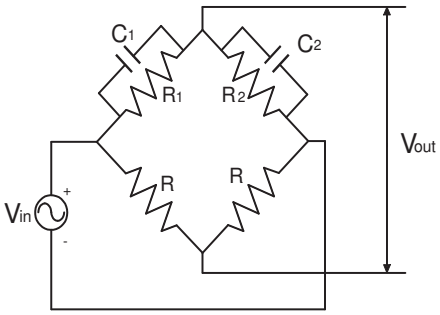

(b)

Fig. 3. (a) Strain gauges and Wheatstone bridge circuit (Half bridge system). (b) Bridge circuit with parasitic capacitance.

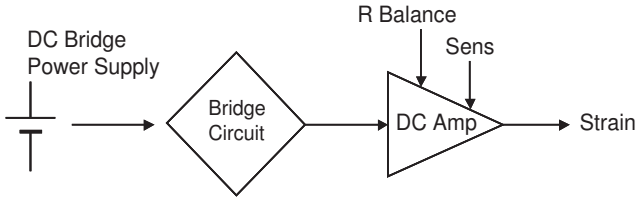

Fig. 4. DC-type dynamic strain measurement system.

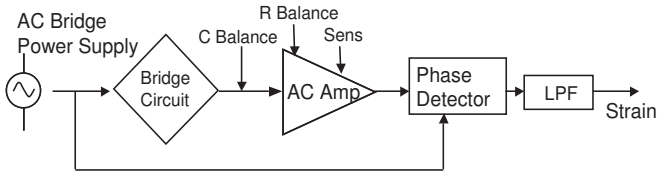

Fig. 5. AC-type dynamic strain measurement system.

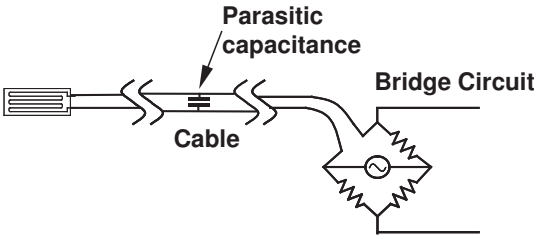

Fig. 6. Strain gauge is located far from the bridge circuit, and they are connected by a cable.

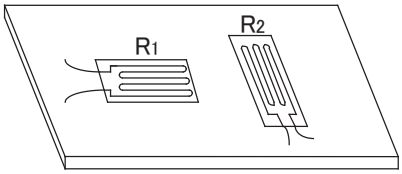

Fig. 7. One strain gauge is attached to the specimen vertically, and the other is attached horizontally.

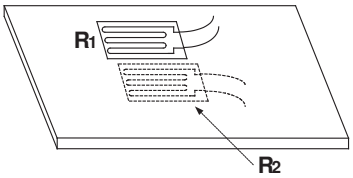

Fig. 8. One strain gauge is attached to the top of the specimen, and the other is attached to its bottom.

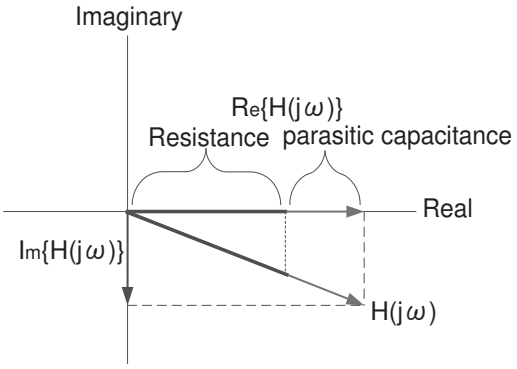

Fig. 9. Effect of parasitic capacitance effects on the real part of $H(j\omega)$.

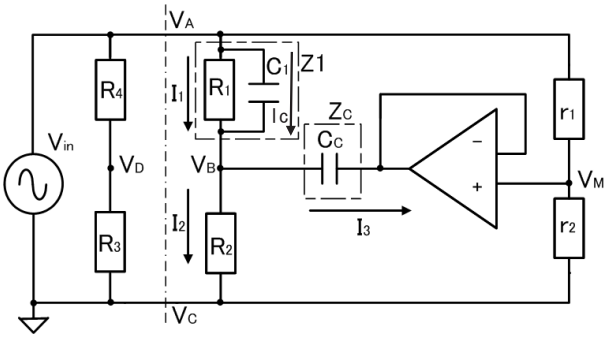

Fig. 10. An analog method for parasitic capacitances C1 compensation.

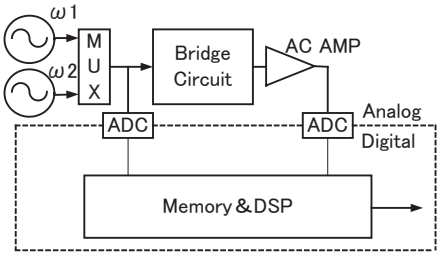

(a)

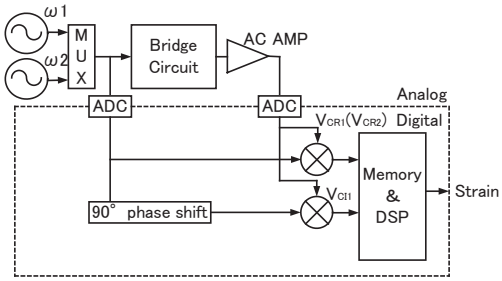

(b)

Fig. 11. (a) Proposed dynamic strain measurement system for a half bridge system. (b) Quadrature phase detection in digital domain.

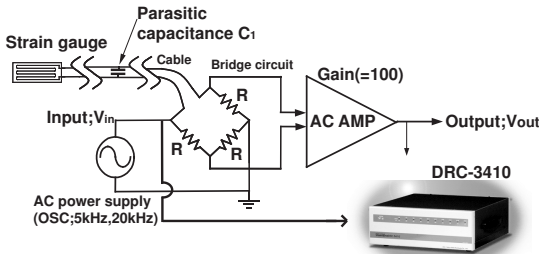

Fig. 12. System for evaluating the proposed algorithm.